# Seasonal cycle and interannual variability in the Amazon hydrologic cycle

Ning Zeng

Department of Atmospheric Sciences and Institute of Geophysics and Planetary Physics
University of California, Los Angeles

**Abstract.** An analysis of the Amazon basin hydrologic cycle has been carried out using the NASA/Goddard Earth Observing System (GEOS-1) atmospheric reanalysis, observed rainfall of *Xie and Arkin* [1996], and historical Amazon River discharge. Over a seasonal cycle the precipitation is found to vary by 5 mm d$^{-1}$, and the runoff is found to vary by 2 mm d$^{-1}$, while the evaporation largely remains constant. On interannual timescales the hydrologic variability both in the atmosphere and at the land surface is found to be closely related to El Niño–Southern Oscillation (ENSO). The correlation between the Southern Oscillation Index and Xie and Arkin precipitation is 0.8 for the period 1985–1993 and 0.56 for the period 1979–1996. The precipitation lags behind the Southern Oscillation Index by 3–4 months while the Amazon River discharge lags behind the precipitation by another 3 months. The lagged relationship suggests interesting dynamic mechanisms. The reanalysis moisture convergence and observed discharge are used to diagnose basin average soil water storage. The year to year variation in the annual mean soil water storage is ~200 mm, comparable to the change within a climatological seasonal cycle. In one case, the basin soil water storage increases by 462 mm from September 1987 to March 1989, suggesting the remarkable ability of the tropical rain forest environment to store and take up water.

## 1. Introduction

Aspects of the hydrologic cycle are of great importance to climate variation and hydrologic applications. Large-scale water budget studies have been conducted for various continental regions [e.g., *Rasmusson*, 1968; *Roads et al.*, 1994]. One crucial aspect of these analyses is the use of atmospheric analysis for closing the water budget at the land surface so the variation in soil water storage can be deduced.

*Matsuyama* [1992] studied the seasonal cycle of the Amazon basin for 1979 and found a 380 mm change in the soil water storage. Such a large water supply plays an important role in sustaining the tropical rain forest environment. *Brubaker et al.* [1993] and *Eltahir and Bras* [1994] analyzed the characteristics of the Amazon hydrologic cycle, especially the role of the precipitation recycling. Amazon rainfall and the runoff of some local rivers are found to be related to the El Niño–Southern Oscillation (ENSO) on interannual timescales [*Ropelewski and Halpert*, 1987; *Marengo et al.*, 1993; *Enfield*, 1996; *Poveda and Mesa*, 1997]. Possible climatic impact of Amazon deforestation involves various aspects of the hydrologic cycle and its interaction with atmospheric dynamics [*Shuttleworth*, 1988; *Zeng and Neelin*, 1999]. The understanding of the present hydrologic cycle and its variation can provide clues for future prediction.

While individual aspects of the seasonal cycle of the Amazon hydrologic cycle have been studied in observations [e.g., *Salati*, 1987; *Shuttleworth*, 1998; *Eltahir and Bras*, 1994; *Wang and Paegle*, 1996] (see above), the water budget for the atmosphere and land as a whole and especially its interannual variability
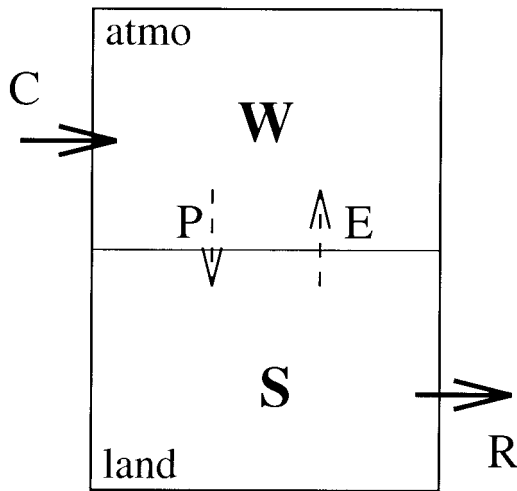
have received less attention. This is partly due to the lack of long-term observations of all the major components of the hydrologic cycle. The atmospheric reanalysis efforts in recent years offer much improved atmospheric statistics without long-term artificial change [e.g., *Schubert et al.*, 1993]. This provides new opportunities for studying the interannual variation of the hydrological cycle. Combined satellite-gauge precipitation data sets have better coverage and accuracy [e.g., *Xie and Arkin*, 1996]. Together with the newly available long-term historical Amazon River discharge data, we address in this paper the large-scale aspects of the Amazon hydrologic cycle using a classical water budget approach. The focus is on its seasonal cycle and interannual variability, both in the atmosphere and at the land surface. In section 2 we describe the data and methodology. In section 3 we analyze the seasonal cycle of the various components of the Amazon hydrologic cycle, followed by an in-depth analysis of its interannual variability in section 4. Conclusions are drawn in section 5.

## 2. Data and Methodology

The NASA/Goddard Space Flight Center (GSFC) Data Assimilation Office Goddard Earth Observing System (GEOS-1) reanalysis [*Schubert et al.*, 1993] is used for analyzing the atmospheric component of the water budget. The data assimilation system employs an optimal interpolation (OI) analysis scheme and the GEOS-1 general circulation model (GCM) with input from in situ and satellite observations. The vertically integrated water vapor flux on the original sigma coordinate is provided, thus avoiding user interpolation on the pressure coordinate, which can result in significant error due to insufficient resolution in the planetary boundary layer. The soil moisture used to evaluate evaporation is calculated off-line on the basis of a simple bucket model driven by monthly mean ob-

**Figure 1.** Conceptual diagram illustrating the vertically integrated water budget in the atmosphere (atmo) and at the land surface. $C$ is moisture convergence, $P$ is precipitation, $E$ is evaporation, $R$ is runoff, $W$ is precipitable water, and $S$ is soil water storage. The dashed lines indicate interior fluxes.

served surface air temperature and precipitation. This influences the partitioning of surface water into runoff and evaporation but does not cause any inconsistency in the atmospheric component. It is not clear whether the results from this off-line approach are better than or not as good as the interactive approach for our purposes. The monthly data are available from March 1985 to November 1993 with horizontal resolution of 2.5° by 2.0°. The model Amazon basin is derived for this resolution from a high-resolution basin boundary data. The area is shaded in Figure 2c.

The monthly historical streamflow records for the Amazon River at Obidos (1°54′S, 55°30′W; drainage area 4,640,300 km$^2$) from 1968 to 1996 and for the Xingu River at Altamira (3°12′S, 52°13′W; drainage area 446,570 km$^2$) from 1968 to 1989 are used to reconstruct the Amazon basin runoff. The streamflow from the River Tapajós, as well as the area near the Amazon River mouth, is not accounted for in the above two station data. The assumption is made that in these regions the runoff rate per unit area (in mm d$^{-1}$) is the same as the average runoff of the drainage area covered by the above two stations. Since the period of available Xingu data does not match the period of the atmospheric data, only its climatology is used, assuming that the interannual variation in the runoff rate for the Xingu drainage area is the same as that for Amazon/Obidos. In order to estimate the possible error of this assumption, we analyzed the data using the reanalysis data for the Amazon basin but excluding the area not covered by the runoff data. We found that the average precipitation is ~5% smaller while the diagnosed seasonal soil water storage (see below for the methodology) has very little change.

The observed precipitation of *Xie and Arkin* [1996] based on gauge and satellite measurements (monthly data at 2.5° by 2.5° resolution available from 1979 to 1996) is used to validate the GEOS-1 reanalysis, and the Southern Oscillation Index (SOI) is adopted as an index for the atmospheric variability over the tropical Pacific Ocean.

The vertically integrated water budget in the atmosphere and at the land surface can be represented by a two-box model (Figure 1). The water budget equation for the atmosphere is

$$\frac{\partial W}{\partial t} = -P + E + C \tag{1}$$

where $W$ is the vertically integrated water vapor (precipitable water), $P$ is precipitation, $E$ is evaporation, and $C$ is the vertically integrated moisture convergence, which can be expressed as

$$C = -\nabla \cdot \mathbf{Q}$$

where $\mathbf{Q}$ is the so-called aerial runoff or water vapor flux:

$$\mathbf{Q} = \frac{P_s}{g} \int_0^1 q\mathbf{v}\, d\sigma$$

where $P_s$ is surface pressure, $g$ is gravity, $q$ is specific humidity, $v$ is wind velocity, and the integral is done in the sigma coordinates from the top of the atmosphere to the surface. The reanalysis also has an analysis increment $A$ on the right-hand side of (1) as the observed data are used to adjust the model prediction. However, it is difficult to allocate this to the three terms in (1) [*Molod et al.*, 1996]. Here we simply neglect $A$, letting the resulting error be absorbed in $C$.

In the land box the water budget equation is

$$\frac{\partial S}{\partial t} = P - E - R \tag{2}$$

where $S$ is the soil water storage and $R$ is the runoff. Possible mismatch between the runoff $R$ as defined here and observed river discharge due to leakage out of the basin will be neglected. Viewing the atmosphere and land surface as one box, the precipitation and evaporation vanish because they are interior fluxes. Mathematically, this is equivalent to combining (1) and (2):

$$\frac{\partial(W + S)}{\partial t} = C - R$$

On the seasonal timescale of concern here the change in the atmospheric precipitable water is quite small (estimated to be <0.1 mm d$^{-1}$), so $\partial W/\partial t$ will be neglected.

Ideally, the water storage $S$ should not change over a long period of time such as several years, so the moisture convergence $C$ should balance the runoff $R$. In analysis this rarely happens owing to inaccuracies in the atmospheric data assimilation system, possible groundwater loss, and other reasons [*Rasmusson*, 1968; *Roads et al.*, 1994]. Therefore a correction is made in the moisture convergence such that

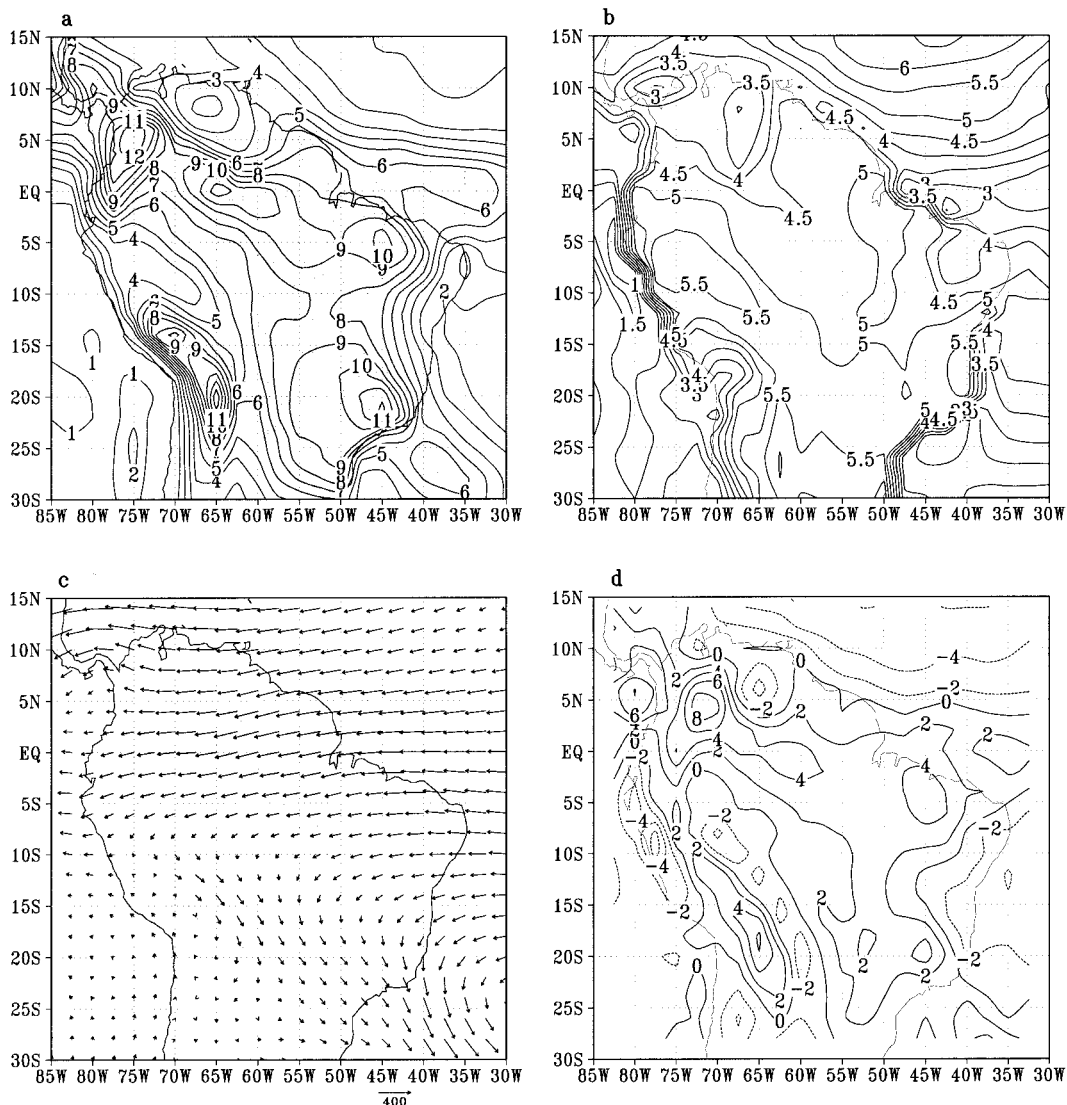$$C^* \equiv C - \bar{C} + \bar{R} \tag{3}$$

where a bar denotes a long-term averaging such that $\bar{C}^* = \bar{R}$ over this period. Without the correction:

$$S = \int_0^t (C^* - R)\, dt + (\bar{C} - \bar{R})t + S_0 \tag{4}$$

where term $(\bar{C} - \bar{R})t$ causes a linear drift with time. An example of this drift is given in section 4. To avoid this drift, we use the corrected water budget equation:

$$\frac{\partial S}{\partial t} = C^* - R \tag{5}$$

and this can be integrated to obtain the soil water storage:

**Figure 2.** Climatological annual mean over the Amazon basin from the NASA/GEOS-1 reanalysis for (a) precipitation, with a contour interval of 1 mm d$^{-1}$, shaded above 4 mm d$^{-1}$; (b) evaporation, with a contour interval of 0.5 mm d$^{-1}$; (c) water vapor flux (kg m$^{-1}$ s$^{-1}$); and (d) moisture convergence, with a contour interval of 2 mm d$^{-1}$. The shaded area in Figure 2c is the model Amazon basin.
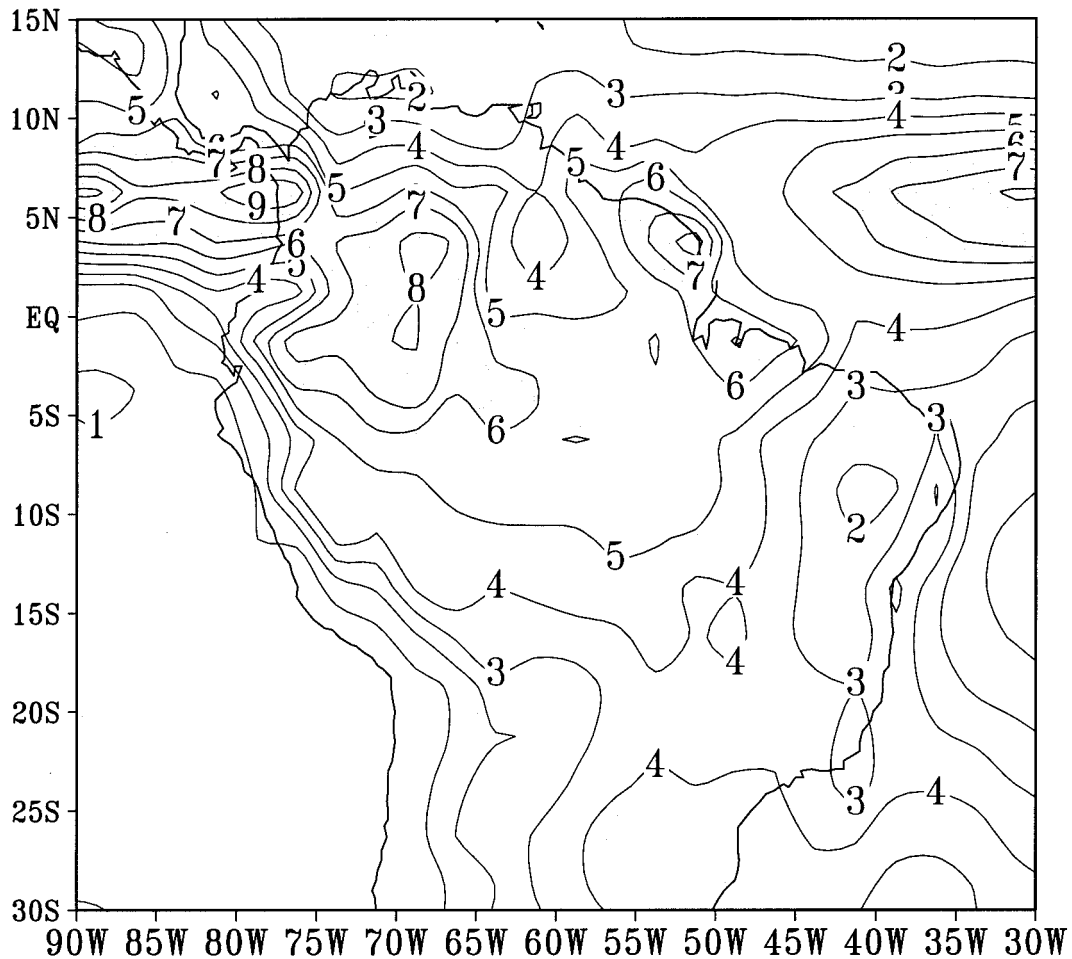
$$S(t) = \int_0^t (C^* - R)\, dt + S_0 \qquad (6)$$

The soil moisture $S$ can only be determined up to an integral constant $S_0$. We choose $S_0$ such that the minimum of $S$ is zero. Equation (6) is used to derive the soil water storage at a time step of 1 month from 1985 to 1993. It is worth noting that the derived $S$ is offset by half a month relative to $C^*$ or $R$ because of the 1 month time step for integration. We choose this offset such that $S$ is centered at the beginning of each month. The 8 year data of all the quantities are then used to derive a climatology. The same period is used for the longer observed rainfall of *Xie and Arkin* [1996] and runoff except in section 4 where we also analyze interannual variability from 1979 to 1996.

## 3. Climatology and Seasonal Cycle

Figure 2 shows the GEOS-1 reanalysis annual mean precipitation, evaporation, moisture flux, and moisture convergence

over the Amazon basin. In general, the reanalysis precipitation has a similar pattern and magnitude compared to the observations of *Xie and Arkin* [1996], shown in Figure 3. A questionable feature is the elongated maximum and minimum along the Andes, likely due to the model's orographic effects [e.g., *Trenberth and Guillemot*, 1995; *Mo and Higgins*, 1996]. This effect is more obvious in the moisture convergence field as moisture divergence occurs over the front valley east of the Andes. The gross pattern of precipitation climatology is found to be similar in a number of other products including the National Centers for Environmental Protection (NCEP)/ National Center for Atmospheric Research (NCAR) reanalysis and the gauge data of Legates and Willmott but with a variance in annual mean rainfall of 6.4% among the six data sets analyzed by *Costa and Foley* [1998, and references therein]. The water vapor flux runs across a large portion of the basin especially in the northern Amazon, with a large outflow bringing the water vapor of Atlantic origin to the Pacific. To the south the flow turns southward, supplying moisture to the
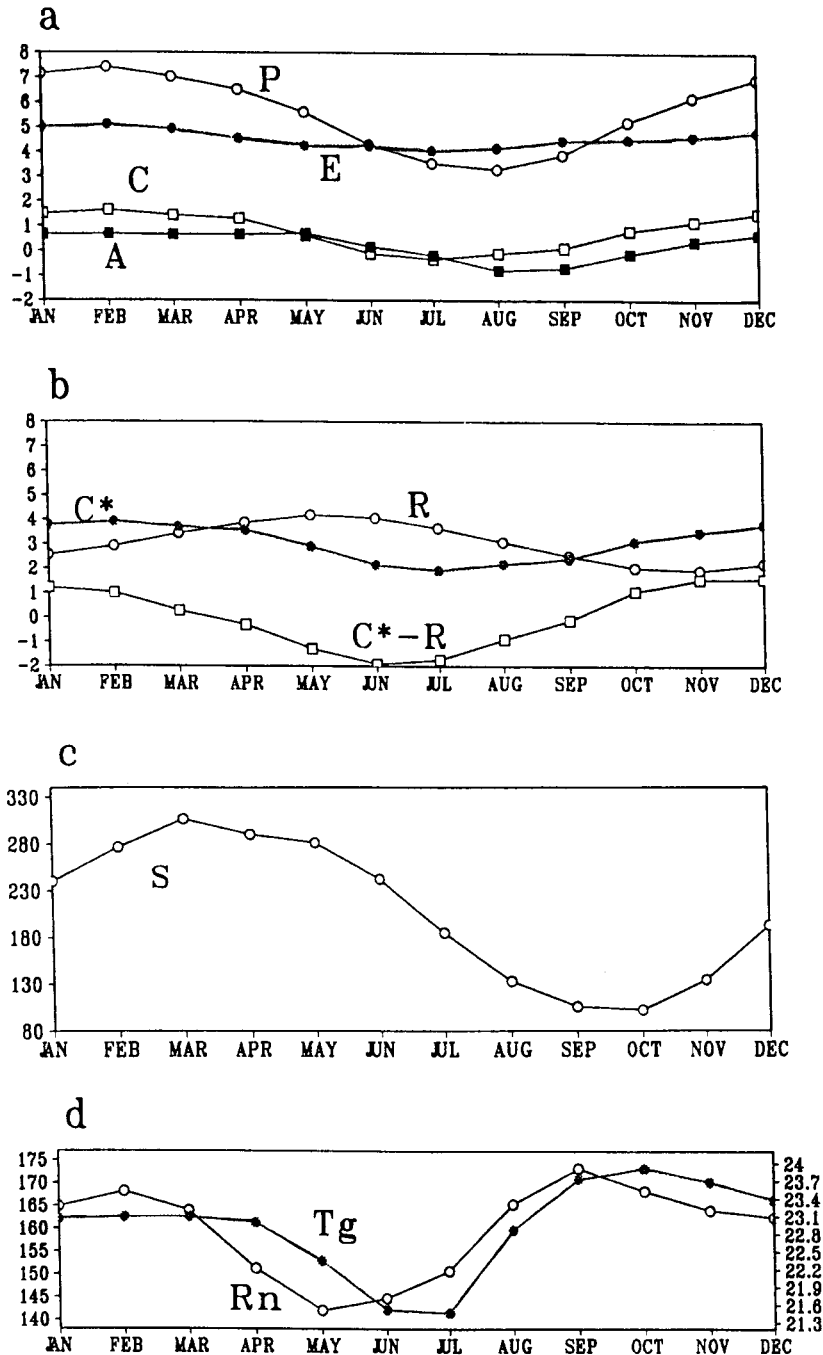
**Figure 3.** Climatological annual mean rainfall of *Xie and Arkin* [1996], with light shading above 4 mm d$^{-1}$ and heavy shading above 6 mm d$^{-1}$.

higher latitudes in South America. Detailed examination season by season seems to indicate somewhat less southward turning compared to the European Centre for Medium-Range Weather Forecasts (ECMWF) analysis [cf. *Eltahir and Bras*, 1994].

The fluxes are averaged over the Amazon basin (shaded in Figure 2c). Since the seasonality is out of phase in the northern and southern Amazon, the basin average tends to be dominated by the southern Amazon because of its larger size. The climatological seasonal cycle of $P$, $E$, $C$, and $P - E - C$ ($\approx$ assimilation increment $A$, since $\partial W/\partial t \approx 0$) is shown in Figure 4a, while *Xie and Arkin* [1996] precipitation is shown in Figure 5. The precipitation shows a profound seasonal cycle with the wet season occurring from January to April, maximizing in February, and the dry season occurring from June to October, minimizing in August. This trend is also seen in the observation, but the dry season in the reanalysis is less dry than it is in the observation. The seasonal amplitude of the reanalysis precipitation is ~1 mm d$^{-1}$ smaller than that of the observation (see below for an estimate of its consequence to the uncertainty in the diagnosed soil water storage). We have further compared both GEOS-1 and the work of Xie and Arkin with long-term station measurements at Manaus. It appears that the Xie and Arkin measurements are quite close to the observations. The agreement in the amplitude is perhaps no surprise since a correction ratio was used in their blended data derived

from the available rain gauge data. The rainfall at a grid point near Manaus from GEOS-1 has a significantly weaker seasonal cycle. However, the basin average of GEOS-1 precipitation is more realistic although it is still too weak (see above). The annual average precipitation from GEOS-1 is 5.6 mm d$^{-1}$, 0.6 mm d$^{-1}$ or 12% larger than that of the observation (Table 1), despite a too small moisture convergence. This is probably related to the high evaporation with an annual mean of 4.6 mm d$^{-1}$, which is too high compared to the 2 year measurement at Manaus of ~3.5 mm d$^{-1}$ [*Shuttleworth*, 1988], if the point observation can be extrapolated to larger spatial scales and longer timescales. The evaporation is relatively constant throughout the year, similar to the measurement at Manaus. The moisture convergence is quite small, with an annual mean of 0.8 mm d$^{-1}$. It displays an annual cycle that closely follows that of precipitation. During the dry season it becomes negative. This is probably not a very realistic feature as is discussed below. The analysis increment ($P - E - C$) also shows a seasonal cycle with positive sign in the wet season and negative sign in the dry season. This differs from what was found in the case of the continental United States [*Schubert et al.*, 1993] where the analysis increment does not show an obvious seasonal cycle.

The annual cycle of runoff for the Amazon basin, deduced from the observed river discharge for the same period (1985–1993), is plotted in Figure 4b. There is an apparent seasonal
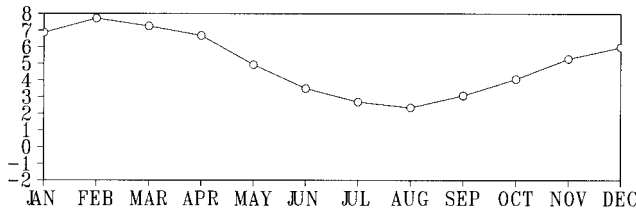
**Figure 4.** Seasonal cycle of basin-averaged Amazon water budget, including (a) precipitation $P$, evaporation $E$, moisture convergence $C$, and $A = P - E - C$ from GEOS-1 reanalysis (mm d$^{-1}$); (b) the observed runoff $R$ and the corrected moisture convergence $C^*$ (mm d$^{-1}$); (c) the diagnosed soil water storage $S$, with the data centered at the beginning of each month (mm); and (d) net radiation $R_n$ (W m$^{-2}$) and ground temperature $T_g$ (K) from GEOS-1 reanalysis.

cycle in runoff. Interestingly, the runoff lags precipitation by about one season, likely owing to the lagged contribution from subsurface drainage since surface runoff tends to occur at a much shorter timescale (e.g., ~2 weeks in the Mississippi River) [*Roads et al.*, 1994]. The annual average runoff is 3.0 mm d$^{-1}$, ~2.2 mm d$^{-1}$ larger than the mean moisture convergence (this difference, $\bar{R} - \bar{C}$, is the correction used for the moisture convergence). If we take the runoff as accurate and consider that over an 8 year period the balance between mois-

ture convergence and runoff should hold reasonably well, this implies a significant underestimation in the reanalysis moisture convergence. Therefore (3) is used to compute a corrected moisture convergence $C^*$, which is then used in (6) to derive the soil water storage $S$, shown in Figure 4c.

The soil water storage has an apparent annual cycle, with an amplitude of ~200 mm. The trend is largely similar to but lags behind precipitation by ~1–2 months. In particular, the soil water storage recovery at the end of the dry season is slow. This

**Figure 5.** Seasonal cycle of Amazon precipitation in mm d$^{-1}$ from *Xie and Arkin* [1996] for the period 1985–1993.

is consistent with the large evaporation the land surface has to supply even during the dry season (equation (2)). *Matsuyama* [1992] found a seasonal change of ~380 mm in the soil water storage for 1979, but he used climatological runoff.

It is worth noting that because the precipitation and evaporation vanish from (5) as interior fluxes, this method of diagnosing soil water storage is not sensitive to uncertainties in these two quantities per se. Furthermore, the correction to the moisture convergence through the balance relation between moisture convergence and runoff reduces systematic errors in the moisture convergence. Thus what is most relevant for the purposes here is the ability of the data assimilation system to simulate the relative seasonal and interannual variability.

Since it is difficult to validate the variation of reanalysis moisture convergence, here we give a rough estimation by assuming that the reanalysis moisture convergence has an error similar to that for the precipitation (a big assumption). Figures 4a and 5 show ~1 mm d$^{-1}$ difference in the seasonal amplitude of precipitation between the reanalysis and *Xie and Arkin* [1996]. We assume that the moisture convergence also has an error with half amplitude $C'_0 = 0.5$ mm d$^{-1}$, and we further assume that the seasonal variation is sinusoidal:

$$C' = C'_0 \cos{(\Omega t)}$$

where $\Omega$ is the angular frequency corresponding to 1 year. Adding this correction term to (5), one can integrate to get its contribution to soil water storage:

$$S' = \frac{C'_0}{\Omega} \sin{(\Omega t)}$$

Given $\Omega = 2\pi/1$ year, this leads to ~60 mm d$^{-1}$ or 30% (60 mm/200 mm) uncertainty in the seasonal amplitude of the diagnosed soil water storage. This is a conservative estimate since the phase of the correction is assumed to be the same as the seasonal cycle.

Also of interest are the surface net radiation $R_n$ and ground temperature $T_g$, shown in Figure 4d. $R_n$ is important in the evaporation process, and $T_g$ is a result of many surface processes [e.g., *Zeng and Neelin*, 1999]. Although there is an apparent annual cycle, the amplitude of $R_n$ is less than 30 W m$^{-2}$, in general agreement with that which was observed at different sites during the Anglo-Brazilian Climate Observational Study (ABRACOS) [*Culf et al.*, 1996], but the overall magnitude is ~30 W m$^{-2}$ larger than the observation. Interestingly, this amount of excessive radiation is just enough to account for the excessive evaporation (see above). The ground temperature shows an annual variation of ~2°C and lags behind $R_n$ by ~1 month. These features are, of course, model dependent. Further observations are needed for better assessment.

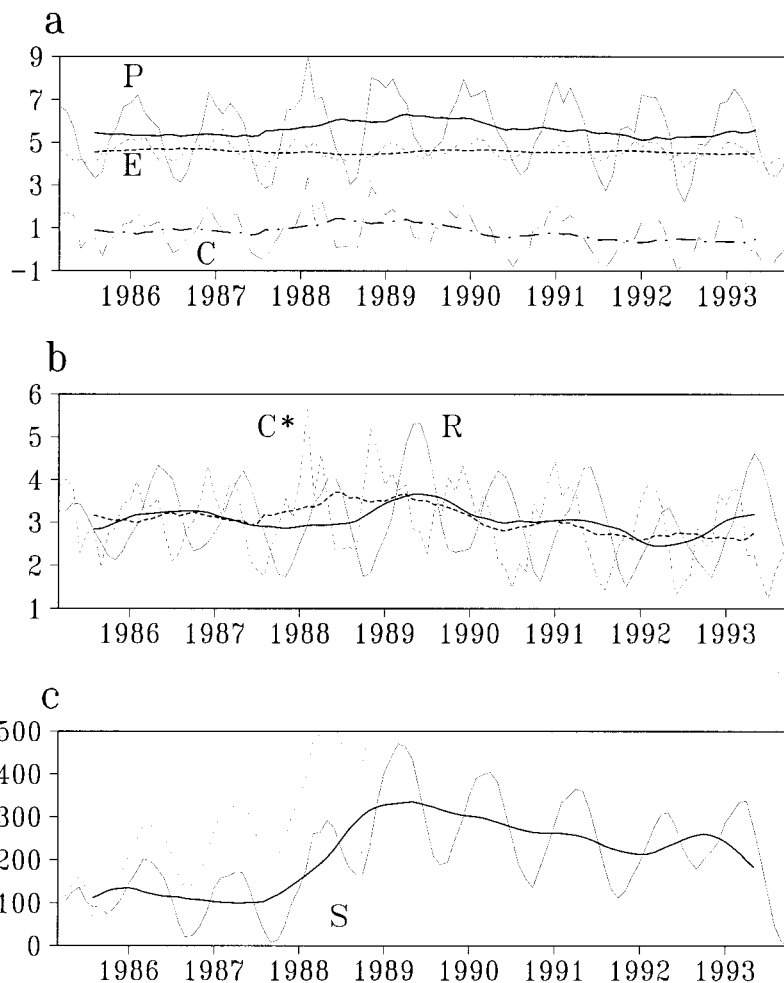## 4. Interannual Variability and Relation to ENSO

The single data assimilation system applied to a long period of time used in the reanalysis is especially suitable for studying interannual variations. Figure 6a shows the monthly values of $P$, $E$, and $C$ and their 12 month running means. Like in the annual cycle, the moisture convergence has a trend similar to that for precipitation. Significant interannual variability in $P$ and $C$ is apparent. The smoothed precipitation (Figure 6a) decreases slightly from 1986 to mid-1987, then increases by 1 mm d$^{-1}$, peaking in spring 1989. This wet period lasted for ~3 years, and the Amazon region is at its low rainfall in early 1992. The evaporation varies only slightly over the whole period.

The observed runoff $R$ and the corrected reanalysis moisture convergence $C^*$, together with their 12 month running means, are shown in Figure 6b; the monthly soil water storage $S$ and its running mean are shown in Figure 6c. The runoff and soil moisture largely follow the precipitation and moisture convergence. The variation in soil water storage $S$ appears to be smoother than that of other fields. The higher-frequency variability is filtered out, likely owing to a buffer effect since $S$ is an integral of the net flux (equation (6)). Nonetheless, the variation in $S$ is large over this period, ~200 mm in the annual average. This is comparable to the mean seasonal variation. In the monthly time series it increases by ~462 mm from September 1987 to March 1989 over a period of 18 months of water recharging. A rapid drop of 350 mm occurs during 1993 within the same year from the wet season to the dry season. *Hodnett et al.* [1996] measured the soil water storage down to a depth of 3.6 m, and they found soil moisture variation ranging from 154 mm at Manaus to 724 mm at Maraba. *Nepstad et al.* [1994] found water extraction of 510 mm down to 8 m depth at an eastern Amazon site during the 1992 dry season. Although the point observations are not directly comparable to the basin average, these results are consistent with the results derived from our water budget analysis. The results demonstrate the large soil water holding capacity and, more impressively, the great ability of the tropical rain forest environment to employ its water storage. The latter is thought to be directly related to the deep roots of tropical plants being able to take up water at depths of 3 m or farther below the surface. Under a deforestation scenario it would be more difficult for short-rooted grass to utilize the deep water storage and thus significantly alter the basin hydrologic cycle. This also indicates that a field capacity of 150 mm, as was used by the bucket model and other earlier land surface parameterization schemes, is not sufficient. Some schemes are now using larger field capacity for the tropical rain forest [e.g., *Randall et al.*, 1996]. The dotted line in Figure 6c illustrates how the linear drift in (4), due to

**Table 1.** Amazon Basin Climatological Annual Means From the Period 1985–1993

| Variable | Annual Mean Value |
|---|---|
| $P$ | 5.6 |
| $E$ | 4.6 |
| $C$ | 0.8 |
| $R$ | 3.0 |
| $P_{\text{Xie}}$ | 5.0 |

$P$, $E$, and $C$ are precipitation, evaporation, and moisture convergence from the GEOS-1 reanalysis. $R$ is runoff from the historical data. $P_{\text{Xie}}$ is the observed precipitation of *Xie and Arkin* [1996]. Units are mm d$^{-1}$.

**Figure 6.** Interannual variations from 1985 to 1993, including (a) precipitation $P$, evaporation $E$, and moisture convergence $C$ from NASA/GEOS-1 reanalysis (mm d$^{-1}$); (b) corrected moisture convergence $C^*$ and observed Amazon basin average runoff $R$ (mm d$^{-1}$); and (c) soil water storage $S$ (mm) diagnosed using equation (6). The thick lines are 12 month running means. The dotted curve in Figure 6c shows the linear drift for a hypothetical imbalance of 0.2 mm d$^{-1}$ between $C$ and $R$ if equation (4) were used.
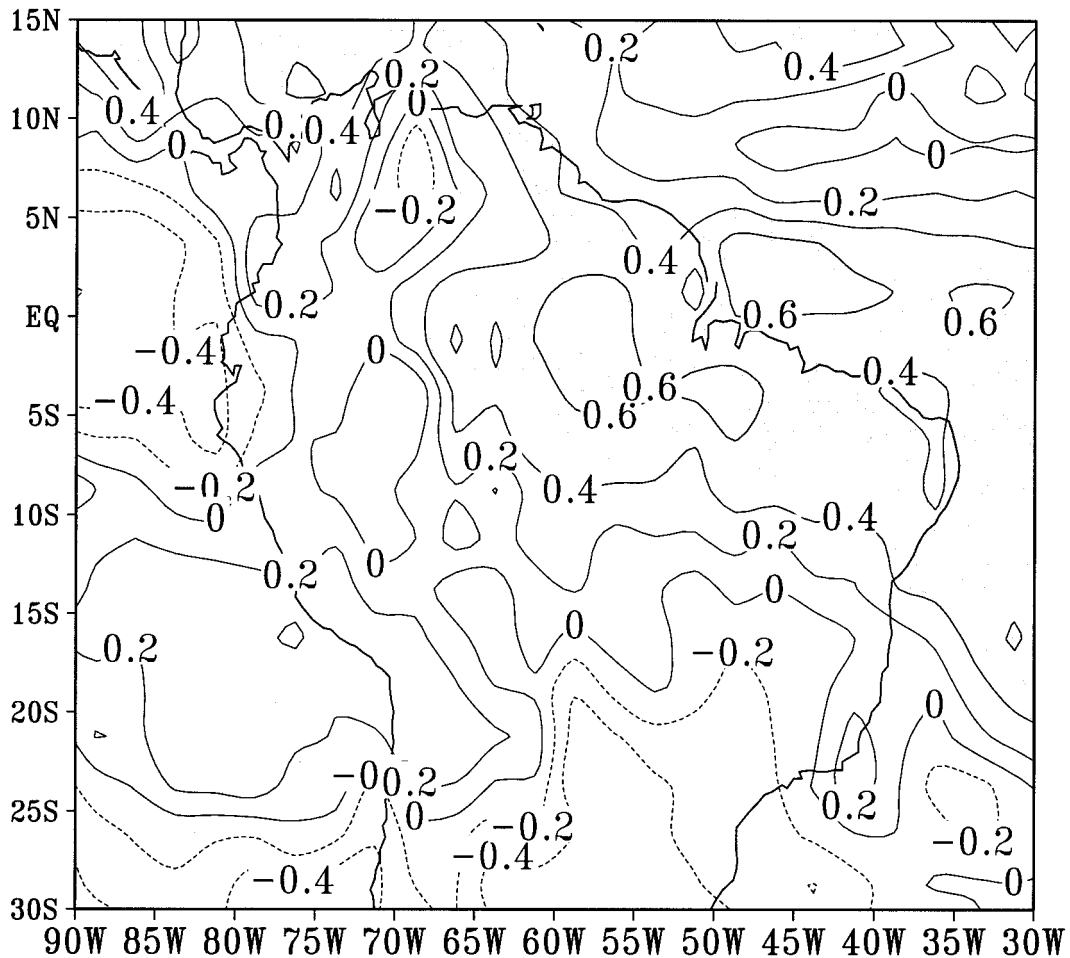
the imbalance in simulated moisture convergence and runoff, can quickly wash away the real signal (in this case, only a small hypothetical imbalance of $\bar{C} - \bar{R} = 0.2$ mm d$^{-1}$ is used; if the actual difference of $-2.2$ mm d$^{-1}$ is used, the curve goes out of the considered range of values in a few months).

The rainfall over the Amazon basin has been found to have a good correlation with El Niño–Southern Oscillation [e.g., *Ropelewski and Halpert*, 1987; *Enfield*, 1996]. A link between streamflow at various rivers and ENSO is also identified [*Richey et al.*, 1989; *Poveda and Mesa*, 1997]. Figure 7 shows the spatial correlations to SOI of *Xie and Arkin* [1996] rainfall for 1979–1996. Correlation between the reanalysis and SOI for 1985–1993 (not shown) shows similar results. A positive correlation of rainfall with SOI is apparent almost everywhere in the Amazon basin, especially in the central and eastern portions. The maximum correlation occurs near the Amazon River mouth with values higher than 0.7. To the south of the basin, negative correlation occurs south of 20°S. This negative correlation is thought to be due to Rossby wave dynamics similar to the Pacific-North America (PNA) pattern. In contrast, the fact that the Amazon basin convection is suppressed during the warm episodes of ENSO is popularly interpreted as

being due to the subsidence induced by a change in the Walker circulation; nonetheless, a generally accepted theory taking into account various feedback processes such as moist convection and cloud radiative effects is lacking.

Figure 8 shows Amazon basin-averaged rainfall of *Xie and Arkin* [1996], SOI, and observed runoff from 1979 to 1996. Also plotted are the reanalysis rainfall in Figure 8b and the diagnosed soil water storage from 1985 to 1993 in Figure 8c. These together with Figure 6 show that the hydrologic cycle of the Amazon basin, both in the atmosphere and at the land surface, is closely related to ENSO. Decreased precipitation, runoff, and soil water are seen during the 1982–1983 and the 1986–1987 warm El Niño events while they increase during the 1988–1989 La Niña event. They then slowly decrease again as the warm event of 1991–1992 approaches. Moderate exceptions occur during 1985 and 1994.

Table 2 lists the correlations of various quantities with SOI. The time series used are 12 month running means from August 1985 to May 1993. The reanalysis precipitation $P$ and moisture convergence $C$ have correlations of 0.78 and 0.81, respectively. The correlation is 0.8 for the observed precipitation, indicating that the reanalysis captures well the interannual variation in

**Figure 7.** Correlation with Southern Oscillation Index (SOI) of *Xie and Arkin* [1996] precipitation for the period 1979–1996, with heavy shading above 0.4 mm d$^{-1}$, light shading below $-0.4$ mm d$^{-1}$, and a contour interval of 0.2 mm d$^{-1}$.

this respect. The runoff $R$ and soil moisture storage $S$ have correlations of 0.56 and 0.53, respectively. Correlations are also computed for the observed precipitation and runoff for the period 1979–1996 (denoted by subscript 7996). They are significantly smaller than those for 1985–1993, indicating differences from event to event. Interestingly, lagged correlation can be seen in the low-pass-filtered precipitation, runoff, and soil water storage (see below).

We have also computed the correlation using only the annual mean. The results are very similar to those obtained using the running mean. It is worth noting that individual months in the running mean are not independent of each other. In a conservative estimate we assign statistical independence only from year to year. A student's $t$ test returns a higher than 99% significance level only at a correlation value greater than 0.8 for the 1985–1993 data (8 degrees of freedom), while it is significant at 99% level for the 1979–1996 data (17 degrees of freedom) at a correlation of 0.6. Undoubtedly, the correlation analysis in this section can be better quantified when longer time series become available.
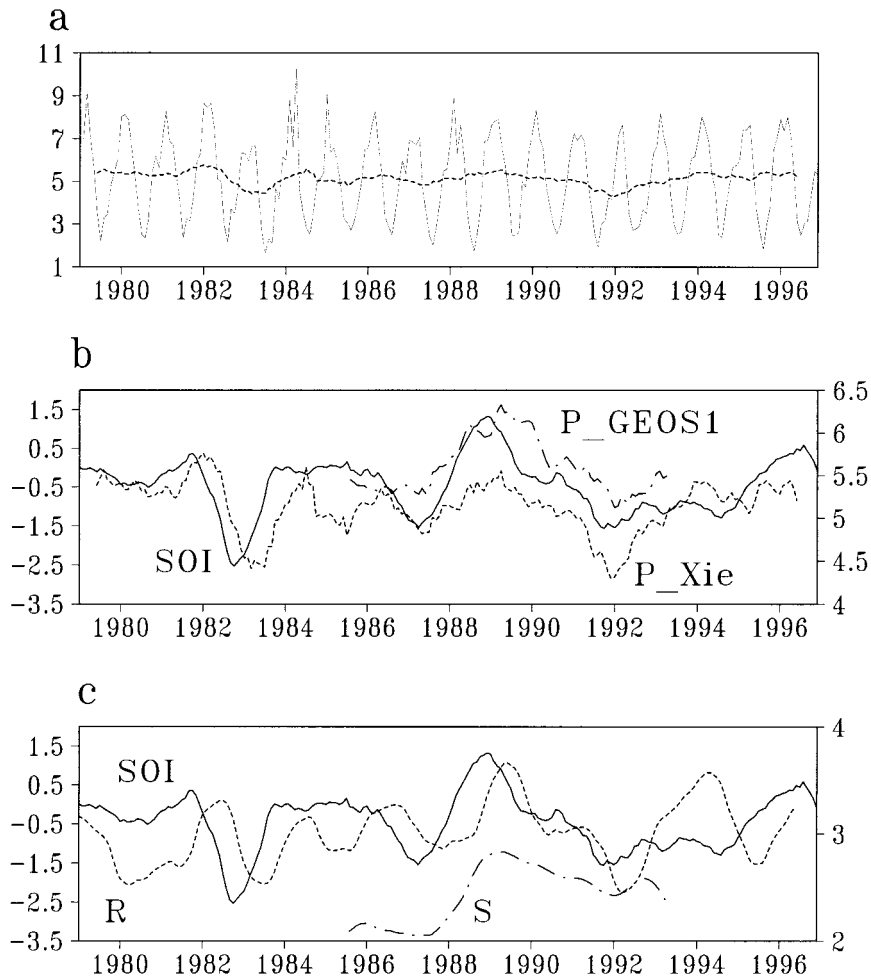
Figure 9 shows the lagged correlations with SOI of the observed rainfall and runoff for the Amazon basin over the period of 1979–1996. It can be seen that the precipitation lags SOI by 3–4 months, while the runoff lags SOI by about 7 months, consistent with the finding of about one season lag of

the runoff behind the precipitation seen in the mean seasonal cycle (section 3). This runoff-rainfall lag indicates a very slow response to precipitation in the subsurface water drainage. The lagged response to SOI in Amazon rainfall is especially pronounced during the 1982–1983 El Niño event but less obvious for the period 1988–1992. This difference from event to event explains why the lag zero rainfall-SOI correlation for the period 1979–1996 is significantly smaller than that for the period 1985–1993 (Table 2), but the correlation increases at a 3–4 month lag (Figure 9). We also computed soil water storage correlation with SOI for 1985–1993 (not shown), which lags rainfall for 1985–1993 by 1–2 months, similar to that which happens in the seasonal cycle (section 3).

## 5. Conclusion

An analysis of the Amazon basin hydrologic cycle has been carried out using the NASA/GEOS-1 reanalysis, observed rainfall, and river discharge data. There exists a profound seasonal cycle in the Amazon hydrologic cycle. On average, the precipitation varies by ~5 mm d$^{-1}$, the runoff varies by ~2 mm d$^{-1}$, and the soil water storage varies by 200 mm, while the evaporation largely remains constant throughout the year. The reanalysis moisture convergence and observed discharge are used to diagnose basin average soil water storage. The year to

**Figure 8.** Plots for the period 1979–1996, including (a) *Xie and Arkin* [1996] precipitation and 12 month running mean (mm d$^{-1}$); (b) 12 month running means of SOI (solid line) in millibars, Xie and Arkin precipitation (dashed line) in mm d$^{-1}$ labeled on the right, and GEOS-1 precipitation (dash-dotted line); and (c) 12 month running means of SOI (solid line), observed runoff $R$ (dashed line) in mm d$^{-1}$ labeled on the right, and diagnosed soil water storage $S$ (dash-dotted line; showing relative magnitude).
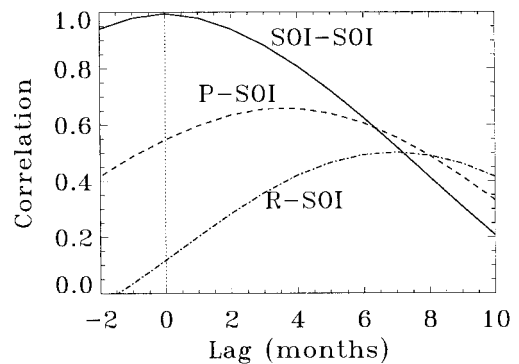
year variation in the annual mean soil water storage is comparable to the change within a climatological seasonal cycle, ~200 mm. In one case, the basin soil water storage increases by 462 mm from September 1987 to March 1989, suggesting the

remarkable ability of the tropical rain forest environment to store and uptake water. After deforestation, it would be more difficult for the short-rooted grass to utilize the deep water storage and thus significantly alter the basin hydrologic cycle.

**Table 2.** Linear Correlation With the Southern Oscillation Index of Various Low-Pass-Filtered Quantities Over the Amazon Basin

| Variable | Linear Correlation |
|---|---|
| $P$ | 0.78 |
| $C$ | 0.81 |
| $R$ | 0.56 |
| $S$ | 0.53 |
| $P_{Xie8593}$ | 0.80 |
| $R_{7996}$ | 0.12 |
| $P_{Xie7996}$ | 0.56 |

Quantities are 12 month running means and include precipitation $P$ and moisture convergence $C$ from the GEOS-1 reanalysis, the historical runoff $R$, the diagnosed soil water storage $S$, and observed rainfall from *Xie and Arkin* [1996]. The correlation coefficients are computed for the period 1985–1993 except $R_{7996}$ and $P_{Xie7996}$, which are for the period 1979–1996.



**Figure 9.** Lagged correlations of *Xie and Arkin* [1996] precipitation $P$ and observed runoff $R$ for Amazon basin with SOI, calculated for the period 1979–1996; positive lag indicates SOI leading.

An estimate indicates that possible errors in the reanalysis moisture convergence can give rise to ~30% uncertainty in the diagnosed soil water storage.

On interannual timescales the hydrological variability both in the atmosphere and at the land surface is found to be closely related to ENSO. The correlation between the Southern Oscillation Index and the observed precipitation is 0.8 for the period 1985–1993 and 0.56 for the period 1979–1996. The latter correlation becomes higher at 0.67 with precipitation lagging SOI by 3–4 months, indicating one season of delay in the response of the Amazon convection to ENSO. This response has an even longer delay during the 1982–1983 El Niño event and the following year of Atlantic warming. The Amazon soil water storage and river runoff further lag the precipitation by 1–2 months and 3 months, respectively. These lagged correlations exist both in the climatological seasonal cycle and in the low-pass-filtered multiyear time series. This lagged relation suggests a delayed response in the Amazon convection to the change in the Pacific Walker circulation. This may involve variations in the Atlantic, as the Atlantic sea surface temperature (SST) tends to lag the Pacific SST [*Enfield and Mayer*, 1997]. On the other hand, this may be simply due to the soil moisture memory. The delayed Amazon convection may then act as a pathway in connecting the Pacific to the Atlantic SST variation in the first place.

Significant uncertainties exist in the results found here which can be sensitive to the data used, in particular, the atmospheric reanalysis data. For instance, despite the correction to the reanalysis moisture convergence (sections 2 and 4), its large bias may lead to significant error through nonlinear effects. Since the land model used in the reanalysis is driven by observed rainfall, the atmosphere and land are not fully coupled. Possible vegetation feedback is not included. It is not totally clear what impacts these would have on the conclusions drawn above. On the other hand, the water budget approach can not be easily replaced by other methods for its capability in diagnosing basin-scale average quantities. Further studies using other reanalysis data can be very useful in narrowing down these uncertainties.

# References

Brubaker, K. L., D. Entekhabi, and P. S. Eagleson, Estimation of continental precipitation recycling, *J. Clim.*, *6*, 1077–1089, 1993.

Costa, M. H., and J. A. Foley, A comparison of precipitation datasets for the Amazon basin, *Geophys. Res. Lett.*, *25*, 155–158, 1998.

Culf, A. D., J. L. Esteves, A. M. Filho, and H. R. da Rocha, Radiation, temperature and humidity over forest and pasture in Amazonia, in *Amazon Deforestation and Climate*, edited by J. H. C. Gash et al., pp. 175–192, John Wiley, New York, 1996.

Eltahir, E. A. B., and R. L. Bras, Precipitation recycling in the Amazon basin, *Q. J. R. Meteorol. Soc.*, *120*, 861–880, 1994.

Enfield, D. B., Relationships of inter-American rainfall to tropical Atlantic and Pacific SST variability, *Geophys. Res. Lett.*, *23*, 3305–3308, 1996.

Enfield, D. B., and D. A. Mayer, Tropical Atlantic sea surface temperature variability and its relation to El Niño-Southern Oscillation, *J. Geophys. Res.*, *102*, 929–945, 1997.

Hodnett, M. G., M. D. Oyama, J. Tomasella, and A. M. Filho, Comparisons of long-term soil water storage behaviour under pasture and forest in the three areas of Amazonia, in *Amazon Deforestation and Climate*, edited by J. H. C. Gash et al., pp. 57–77, John Wiley, New York, 1996.

Marengo, J. A., L. M. Druyan, and S. Hastenrath, Observational and modeling studies of Amazonia interannual climate variability, *Clim. Change*, *23*, 267–286, 1993.

Matsuyama, H., The water budget in the Amazon river basin during the FGGE period, *J. Meteorol. Soc. Jpn.*, *70*, 1071–1083, 1992.

Mo, K. C., and R. W. Higgins, Large-scale atmospheric moisture transport as evaluated in the NCEP/NCAR and the NASA/DAO reanalysis, *J. Clim.*, *9*, 1531–1545, 1996.

Molod, A., H. M. Helfand, and L. L. Takacs, The climatology of parameterized physical processes in the GEOS-1 GCM and their impact on the GEOS-1 data assimilation system, *J. Clim.*, *9*, 764–785, 1996.

Nepstad, D. C., et al., The role of deep roots in the hydrological and carbon cycles of Amazonian forests and pastures, *Nature*, *372*, 666–669, 1994.

Poveda, G., and O. J. Mesa, Feedbacks between hydrological processes in tropical South America and large-scale ocean-atmosphere phenomena, *J. Clim.*, *10*, 2690–2702, 1997.

Randall, D. A., et al., A revised land surface parameterization (SIB2) for GCMs, 3, The greening of the Colorado State University General Circulation Model, *J. Clim.*, *9*, 738–763, 1996.

Rasmusson, E. M., Atmospheric water vapor transport and the water balance of North America, II, Large-scale water balance investigation, *Mon. Weather Rev.*, *96*, 720–734, 1968.

Richey, J. E., C. Nobre, and C. Deser, Amazon river discharge and climate variability: 1903 to 1985, *Science*, *246*, 101–103, 1989.

Roads, J. O., S.-C. Chen, A. K. Guetter, and K. P. Georgakakos, Large-scale aspects of the United States hydrologic cycle, *Bull. Am. Meteorol. Soc.*, *75*, 1589–1610, 1994.

Ropelewski, C. F., and M. S. Halpert, Global and regional scale precipitation associated with El Niño/Southern Oscillation, *Mon. Weather Rev.*, *115*, 1606–1626, 1987.

Salati, E., The forest and the hydrological cycle, in *The Geophysiology of Amazonia: Vegetation and Climate Interactions*, edited by R. E. Dickinson, pp. 273–296, John Wiley, New York, 1987.

Schubert, S. D., R. B. Rood, and J. P. Pfaendtner, An assimilated dataset for earth science applications, *Bull. Am. Meteorol. Soc.*, *74*, 2331–2342, 1993.

Shuttleworth, W. J., Evaporation from Amazonian rain forest, *Proc. R. Soc. London, Ser. B*, *233*, 321–346, 1988.

Trenberth, K. E., and C. J. Guillemot, Evaluation of the atmospheric moisture budget as seen from analyses, *J. Clim.*, *8*, 2255–2272, 1995.

Wang, M. Y., and J. Paegle, Impact of analysis uncertainty upon regional atmospheric moisture flux, *J. Geophys. Res.*, *101*, 7291–7303, 1996.

Xie, P., and P. A. Arkin, Analyses of global monthly precipitation using gauge observations, satellite estimates, and numerical model predictions, *J. Clim.*, *9*, 840–858, 1996.

Zeng, N., and J. D. Neelin, A land-atmosphere interaction theory for the tropical deforestation problem, *J. Clim.*, *12*, 857–872, 1999.

N. Zeng, Department of Atmospheric Sciences, University of California, Los Angeles, CA 90095-1565. (zeng@atmos.ucla.edu)